BULLETIN OF THE CHEMICAL SOCIETY OF JAPAN VOL. 42 2820—2827 (1969)

Electrophotographic Properties of Titanium-Dioxide Resin Dispersion Layers

Takeaki IIDA and Hiroshi NOZAKI

The Institute of Industrial Science, The University of Tokyo, Roppongi, Minato-ku, Tokyo

(Received April 15, 1969)

The electrophotographic properties of titanium dioxide-polymer dispersion layers were studied. The titanium dioxide powder of the rutile type and three well-known polymers, polyvinyl acetate, polyvinyl chloride, and polystyrene, were used. The measurements were done on the corona-charging properties, *e. g.*, the resistivity and the capacitance of the layer, the rising gradient of the surface potential, and the fatigue effect of pre-illumination. The results make it clear that the analysis of an equivalent circuit can be applied to the interpretation of the rising gradient of the surface potential and to that of the dark decay to some extent. Moreover, it is found that the logarithm of the potential of the dark decay decreases proportionally to the cube root of the time at the initial step, while, at the next following step, it decays proportionally to the square root of the time. The mechanism of the dark decay of the surface potential is also discussed.

Titanium dioxide is famous as a white pigment, and it is one of the compounds of the transition elements. Therefore, this material has many interesting properties; for example, titanium dioxide ceramics have a high dielectric constant (114), and titanium dioxide has a photoconductivity at the wavelength of around 410 mμ.[1] At first we used this material as a photoconductor. Then we

have developed an Electrofax method,[2] in which titanium dioxide was used as a photoconductor instead of zinc oxide; we have obtained many good results with this method. Moreover, the image quality could thus be improved to the same quality as that of the zinc-oxide paper.

On the other hand, in the Electrostatic Recording method, a quite new application has recently been discovered;[3] that is, the addition of titanium dioxide to the recording paper improves the image quality of the electrostatic recording process, in which a pin tube is used as the recording head.[4] It is considered that the electrical capacity of the recording layer is increased by the addition of titanium dioxide; the real impedance of the layer against a pulse signal is then decreased. It results that an electron beam emitted from the pin head can easily pass through the recording paper, and the tailing phenomenon of a signal,[5] which is caused by the residual potential at the pin head, decreases greatly. Then the signal-to-noise ratio of the image is increased and the image quality is improved. The electrostatic recording methods have been applied in many fields, *e. g.*, in making of the facsimiles of newspapers, in the recording method of an electronic computer,[6] in the recording of TV images,[7] and in the use of an electrostatic printer.[8]

In view of these points, it is very important to study the electrophotographic properties of the dispersion layer of titanium dioxide. The electrophotographic properties of the zinc oxide-resin dispersion layer were studied by Inoue[9] and by Tashiro *et al.*,[10] and the mechanism of the corona charging was discussed by Amick[11] to some extent. Therefore, we investigated the electrophotographic properties of the titanium dioxide-resin dispersion layer on various titanium-dioxide contents. We believe that these studies will contribute as fundamental data to the industrial applications of the Electrostatic Recording technique.

Experimental

Sample. *Titanium Dioxide.* Titanium dioxide powder of the rutile type was produced by the hydrolysis of titanium tetrachloride.[12] The purity of this powder corresponded to spectro grade. The major impurities detected by chemical analysis were as follows: Fe, less than 0.005%, As, less than 0.0005%, and Pb, less than 0.002%. The average crystal size of this powder was from 0.2 to 0.7μ. The specific surface area of this powder, as determined by the B.E.T. method, was 1.57 m^2/g.

Organic Polymers. These were used as a powder's binder. In order to make an experiment on a definite

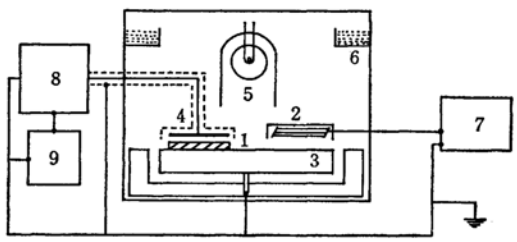

Fig. 1. The block diagram of the experimental equipment.
(1) dispersion layer, (2) steel wand for corona discharge, (3) turn-table, (4) detector, (5) tungsten light, (6) silicagel powder, (7) electric source of high voltage, (8) surface potentialmeter of chopper type, (9) electrical recorder.

Table 1. The properties of the polymers

Polymer	Mean degree of polymerization	Mean molecular weight	Dielectric constant (at 1 kc)	Dipole moment (Debye unit, at 20°C)
Polyvinyl acetate (P. V. Ac.)	1400	100000	5.2	1.68[13]
Polyvinyl chloride (P. V. C.)	1300	80000	4.5	1.62[14]
Polystyrene (P. S.)	1400	130000	2.4	0.26[15]

1) T. Iida and H. Nozaki, This Bulletin, **42**, 929 (1969).
2) H. Nozaki, Manuscrips for 1st International Congress on Reprography, Köln (1963); H. Nozaki and T. Iida, Manuscrips for 2nd International Congress on Reprography, Köln (1967).
3) S. Matsui and Y. Higaki, Manuscrips for 22nd Congress of Electrophotographic Soc. Japan, 1968.
4) S. Matsui, *Electrophotography*, **7**, 94 (1967).
5) S. Matsui, Manuscrips for 20th Congress of Electrophotographic Soc. Japan, 1967.
6) J. Hojo, *Electrophotography*, **7**, 117 (1967).
7) S. Kineri and Y. Okajima, *ibid.*, **7**, 151 (1967).
8) K. Kobayashi, H. Ohta, Y. Okajima and S. Nanba, *ibid.*, **7**, 105 (1967).
9) E. Inoue, H. Kokado, T. Yamaguchi, S. Nagashima and K. Takahashi, *ibid.*, **1**, 27 (1959).
10) I. Tashiro, T. Kimura, M. Kuwahara and G. Ohno, *ibid.*, **8**, 3 (1967).
11) J. A. Amick, *RCA Rev.*, *Dec.*, 753, 770 (1959).
12) T. Iida and H. Nozaki, *Kogyo Kagaku Zasshi (J. Chem. Soc. Japan, Ind. Chem. Sect.)*, **69**, 2087 (1966).
13) A. Kodera, *Kagaku*, **10**, 81 (1955).
14) P. Debye and F. Bueche, *J. Chem. Phys.*, **19**, 589 (1951).
15) O. Broen and F. H. Muller, *Kolloid-Z.*, **140**, 121 (1955); *ibid.*, **141**, 20 (1956).

system, pure polymers were used. The properties of these polymers are shown in Table 1.

Solvents. Solvents purified by repeated distillations were used; ethyl acetate was used for polyvinyl acetate; cyclohexanone, for polyvinyl chloride, and benzene, for polystyrene.

Procedures for Making the Dispersion Layer. The powder of titanium dioxide and the polymer solution were mixed in a blender for ten hours. The suspension of these materials was coated uniformly on a domestic aluminium foil (7 cm × 10 cm) by means of a film applicator of the Baker type. These specimens were dried at 110°C for two hours, and then they were preserved in a dark chamber for 48 hr or more; the relative humidity was controlled at about 20%, and the temperature was between 15 and 25°C. The thickness of the coated layer was between 15 and 20 microns. The weight of the titanium dioxide against the weight of the polymer changed between 0% and 90%.

The Measurement of the Electrical Resistivity and the Electrostatic Capacity of the Disperison Layer. At first silver metal was evaporated with a vacuum evaporator on the layer surface. This specimen was fixed in a dark chamber in which the relative humidity was controlled with a silica gel powder. An electrode of stainless steel was put on the sample surface. The weight of the electrode was 10.0 g/cm². The electrical resistivity was directly measured with a Keithley electrometer of the 610-B type. The electrostatic capacity was measured with a Wheatstone's bridge, applying an alternative current of 1 kc.

The Measurement of the Corona-charging Potential. The measurement was done by the turn-table method. A block diagram of the experimental equipment is shown in Fig. 1.

All the measurements were done at room temperature in air with a relative humidity of about 20%. The table was rotated at a speed of 78 rpm; the surface potential was measured with a surface potentialmeter of the chopper type, and the corona discharge was done with three steel wands, 0.1 mm in diameter, which were fixed 5 mm above the turn-table. The conditions of the corona discharge were as follows: the discharge voltages were −6.0 kV and 6.5 kV at the negative and at the positive corona discharge respectively; the current of the corona discharge was maintained at a constant current of 4.2×10^{-5} A and the corona discharge was done for one minute. After the dark decay had been observed for one minute, the tungsten light of 200 lux at the sample surface was lighted until the surface potential disappeared. In the case of the measurement of the light-fatigue effect, the sample was irradiated with a tungsten light of 1200 lux for two minutes, and then, the above measurements were made. The potential change was recorded with an electrical recorder, as is shown in Fig. 1. One of the examples of the potential change against the time is shown in Fig. 2. The full line corresponds to the surface potential on fresh layers, and the dotted line, to the surface potential measured after irradiation with a light of 1200 lux for two minutes as a pre-illumination.

The notations of the electrophotographic properties are shown in Table 2.

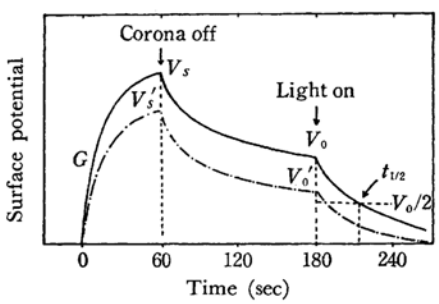

Fig. 2. The time dependence of the surface potential of the corona charging.

TABLE 2. SYMBOLS

Notation	Unit	Meaning
V_s	volt	saturation surface potential
E_s	volt/μ	saturation potential per one micron thickness
V_0	volt	initial surface potential
G	volt/sec	rising gradient of surface potential
$t_{1/2}$	sec	half-time of light decay
V_0/V_s	—	quantity of dark decay
V'_s/V_s	—	quantity of fatigue effect by pre-illumination

Results

The specific resistivity of the dispersion layer decreases with an increase in the titanium-dioxide contents, as is shown in Fig. 3. The resistivity of these dispersion layers is situated between 10^{13} and 10^{15} Ω cm. The polystyrene dispersion layer has the highest resistivity, while the polyvinyl acetate layer has the lowest resistivity. Each curve has a minimum resistivity at around 50% of the titanium-dioxide contents.

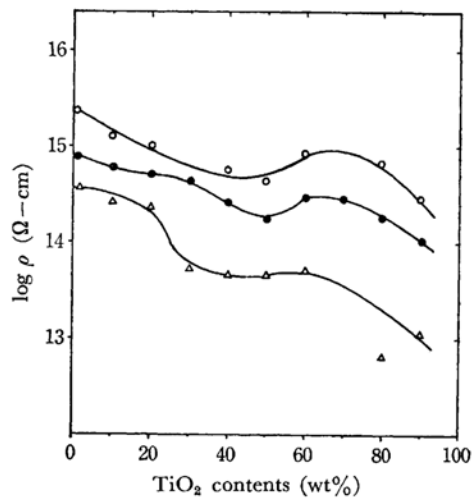

Fig. 3. Relations between the specific resistivity of the dispersion layer and the titanium-dioxide contents.
○ P. S. ● P. V. C. △ P. V. Ac.

The electrostatic capacities of the dispersion layer are plotted against the contents of titanium dioxide. The capacity was calculated with the normalization of a unit area of 1 cm² and of a unit thickness of one micron. As can be seen in Fig. 4, the capacity of the plyvinyl acetate layer is the highest, while that of the polyvinyl chloride layer is slightly lower than that of the polyvinyl acetate layer. The capacity of the polystyrene layer has the lowest value of the three. The dielectric constants of the rutile ceramics is 114, but that of these dispersion layers of the titanium-dioxide contents of between 80% and 90% takes a value as small as between 30 and 40. The dielectric constants gradually decreases with a decrease in the titanium-dioxide contents.

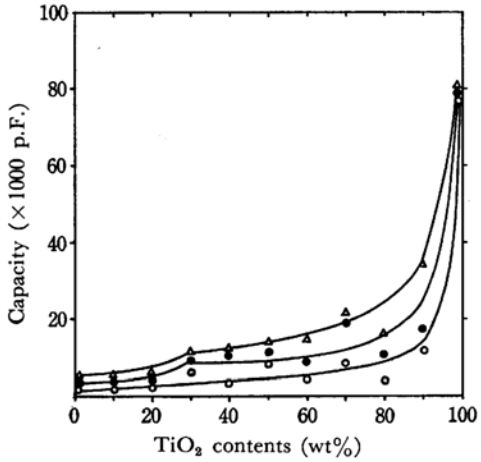

Fig. 4. Relations between the electrostatic capacity of the dispersion layer and the titanium-dioxide contents.
△ P. V. Ac. ● P. V. C. ○ P. S.

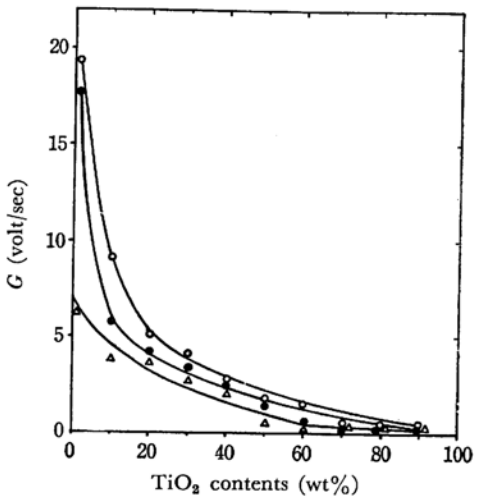

Fig. 5. The rising gradients of the surface potential plotted against the titanium-dioxide contents.
○ P. S. ● P. V. C. △ P. V. Ac.

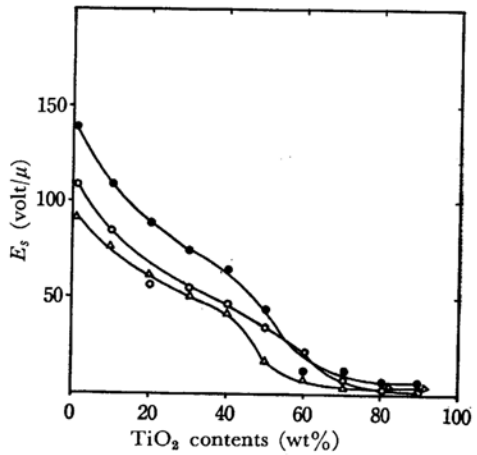

Fig. 6. The relations between the saturation potential per one micron thickness and the titanium-dioxide contens.
● P. V. C. ○ P. S. △ P. V.

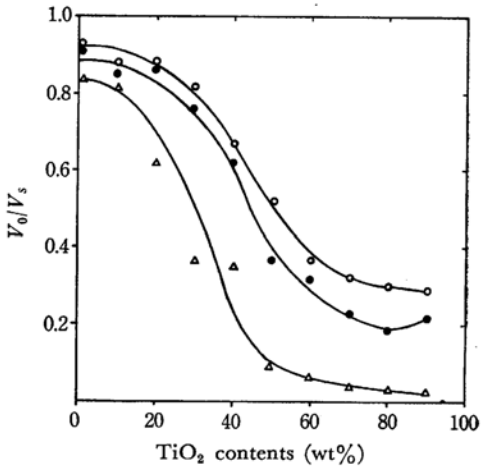

Fig. 7. The quantity of the dark decay measured one minute after the turn off of the corona discharge.
○ P. S. ● P. V. C. △ P. V. Ac.

The corona charging was done with both the negative and the positive corona discharging, but in the case of the titanium-dioxide dispersion layer, the potential of the positive corona charging can hardly be observed. Therefore, all the following results are the properties of the negative corona charging.

The rising gradients of the surface potential in the negative corona charging decrease with an increase in the titanium-dioxide contents. The rising gradients of the surface potential are plotted against the titanium-dioxide contents in Fig. 5. The order of the rising gradients of these dispersion layers is as follows: the polystyrene dispersion layer>the polyvinyl chloride dispersion layer>the polyvinyl acetate dispersion layer.

The relations between the saturation potential of the negative corona charging per micron of thickness and the titanium-dioxide contents are shown in Fig. 6. The saturation potential decreases with an increase in the titanium-dioxide contents. The polyvinyl chloride layer takes the value of the highest potential; the next is the polystyrene layer, and the polyvinyl acetate layer takes the smallest potential.

The quantities of the dark decay, measured one minute after the turn-off of the corona discharge, are shown in Fig. 7. The dark decay increases with an increase in the titanium-dioxide contents. The polystyrene layer has the slowest decay, and the polyvinyl acetate has the quickest.

The half-time of the light decay decreases with an increase in the titanium-dioxide contents, as is shown in Fig. 8. At the lower contents of titanium dioxide of between 0% and 30%, the order of the speed of the light decay is as follows: the polystyrene dispersion layer > the polyvinyl acetate dispersion layer > the polyvinyl chloride dispersion layer. At high contents of titanium dioxide (between 40% and 90%), no clear differences in the light decay are detected among these dispersion layers.

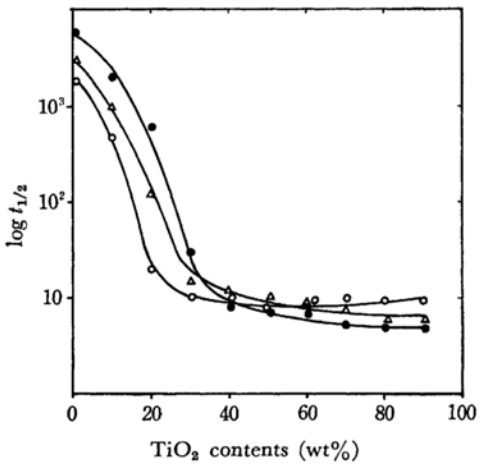

Fig. 8. The logarithm of the half-time of the light decay plotted against the titanium-dioxide contents.
○ P. S. △ P. V. Ac. ● P. V. C.

The quantities of the fatigue effect produced by pre-illumination are shown in Fig. 9. As can be seen in the figure, the fatigue effects of the polyvinyl acetate layer and the polyvinyl chloride layer increase with an increase in the titanium-dioxide contents, reaching a maximum at contents of around 80%. However, the fatigue effect of the polystyrene layer is somewhat different from the former two binders; it has its maximum at contents of around 40%.

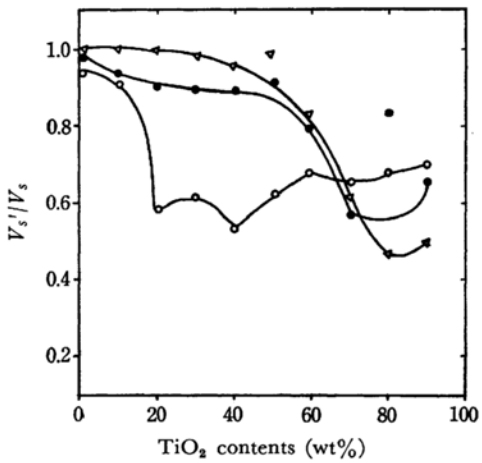

Fig. 9. The quantity of the fatigue effect by a pre-illumination.
△ P. V. Ac. ● P. V. C. ○ P. S.

The relations between the logarithm of the surface potential in the dark decay and the square root of the time, which were measured in the case of 0% contents of titanium dioxide, are shown in Fig. 10. In the region from 1 min to 9 min, the surface potential does not decay proportionally to the square root of the time, but in the region from 9 min to 80 min the surface potential does decay so. The decay gradient of $-\mathrm{d}\log V/\mathrm{d}t^{1/2}$ are evaluated as follows: the polyvinyl chloride layer is 0.216, the polystyrene layer is 0.316, and the polyvinyl acetate layer is 0.533.

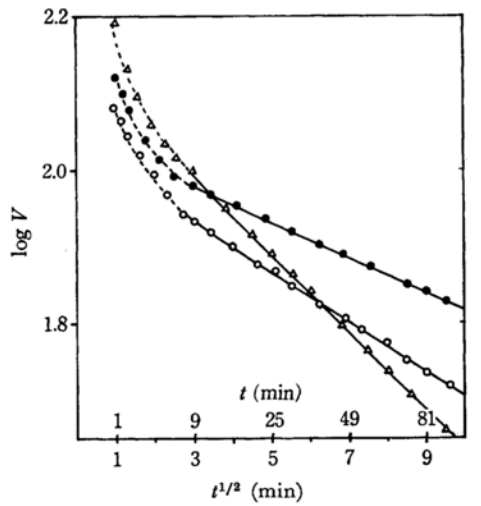

Fig. 10. The relations between the logarithm of the dark decay potential on the polymer layer of 0% titanium-dioxide contents and the square root of the time.
Polymer 100% ● P. V. C.
○ P. S.
△ P. V. Ac.

The same measurements were made on the dispersion layers of 30% contents of titanium dioxide. the results are shown in Fig. 11. In this case the proportionality between the logarithm of the surface potential in the dark decay and the square root of the time starts about six minutes after the turn-off of the corona discharge.

As has been mentioned above in discussing the results of Fig. 10, the logarithm of the surface potential does not decay proportionally to the square root of the time in the region from 1 min to 9 min. Therefore, we tried to plot the logarithm of the potential decay of this region against the cube root of the time. The results are shown in Fig. 12. As can be seen in the figure, the logarithm of the surface potential does indeed decay proportionally to the cube root of the time.

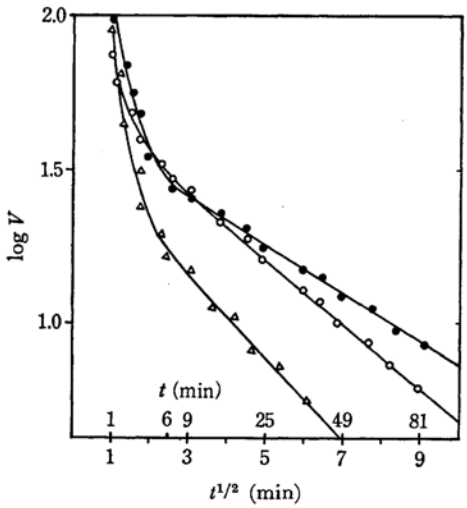

Fig. 11. The relations between the logarithm of the dark decay potential on the dispersion layer of 30% titanium-dioxide contents and the square root of the time.
● P. V. C.
TiO_2 30% ○ P. S.
△ P. V. Ac.

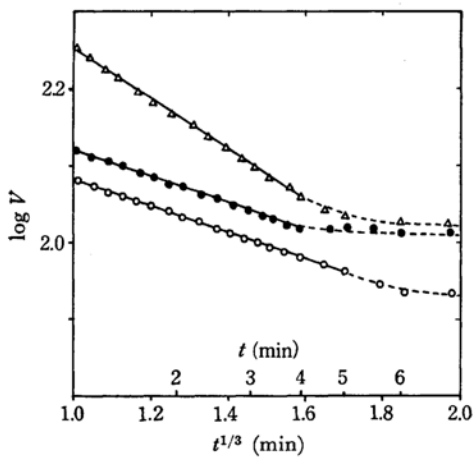

Fig. 12. The relations between the logarithm of the dark decay potential at the initial step and the cube root of the time.
Polymer 100% △ P. V. Ac.
● P. V. C.
○ P. S.

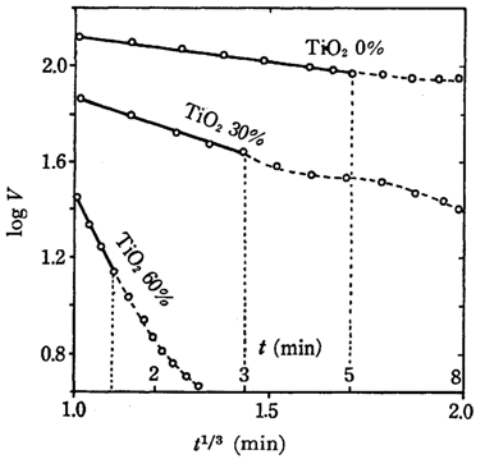

Fig. 13. The relations between the logarithm of the dark decay potential at the initial step on the polystyrene dispersion layer of the various titanium dioxide contents and the cube root of the time.

The period for which the proportionality of the relation between log V and $t^{1/3}$ is retained depends on the contents of titanium dioxide. As an example, the relations between the log V and $t^{1/3}$ of the polystyrene layer at various titanium-dioxide contents are shown in Fig. 13. The polystyrene layer of 0% contents of titanium dioxide retains the proportionality for 5.0 min, that of 30% contents of titanium dioxide does so for 3.0 min, and that of 60% contents of titanium dioxide does so for 1.5 min. Therefore, it is found that the period of the proportionality decreases with an increase in the titanium-dioxide contents.

Discussion

The charging properties were studied by the use of three different polymers, and it was found that the charging properties depend considerably on the polymer used as a binder. As is shown in Table 1, the mean degrees of polymerization and the molecular weights of these polymers are not very different, but the dielectric constants and the dipole moments of these polymers are quite different. A polymer which has a high dipole moment generally has a high dielectric constant. It is quite reasonable that a layer's capacity, as measured by direct measurements, increases with an increase in the dielectric constant of the polymer, as is shown in Fig. 4. Moreover, the resistivity of the layers is

shown in Fig. 3. We can, therefore, see the resistivity and the capacity of the layer. It is reasonable to explain these charging properties qualitatively with the use of an equivalent circuit, which is shown in Fig. 14.

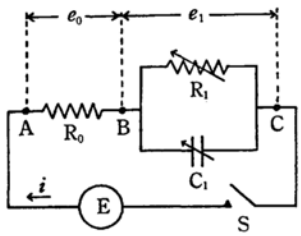

Fig. 14. The equivalent circuit of the dispersion layer in the corona charging process.
e_0: potential difference between A and B
e_1: potential difference between B and C
R_0: resistance of the circuit
R_1: variable resistance which corresponds to the resistance of the layer
C_1: variable capacity which corresponds to the capacity of the layer
E: electric source
S: switch

When the switch, S, is turned on, and a voltage, E, is applied to the circuit, the change in the potential between B and C is derived as the following equation:

$$e_1 = \frac{ER_1}{R_0 + R_1}\left[1 - \exp\left\{-\frac{1}{C_1}\left(\frac{1}{R_0} + \frac{1}{R_1}\right)t\right\}\right] \quad (1)$$

When e_1 is differentiated by the time, the rising gradient of the potential between B and C is obtained:

$$G = \frac{de_1}{dt} = \frac{ER_1^2C_1R_0}{(R_0 + R_1)^2}\exp\left\{-\frac{1}{C_1}\left(\frac{1}{R_0} + \frac{1}{R_1}\right)t\right\} \quad (2)$$

From Eq. (2) it can be deduced that G decreases with an increase in C_1, if R_1 is kept as a constant value. It can also be deduced from Eq. (2) that G decreases with an increase in R_1 if C_1 is kept as a constant value. As is shown in Fig. 5, the order of G is as follows: the polystyrene dispersion layer> the polyvinyl chloride dispersion layer>the polyvinyl acetate dispersion layer. This means that the rising gradient of the corona charging decreases with an increase in the capacity of the layer. Therefore, it can be clarified that the rising gradient of the corona charging depends greatly on the capacitance of the layer.

In the case of the discharging process, when the switch is turned off the potential between B and C decreases, because the discharging current flows through the resistance of R_1. Therefore, the speed of the dark decay of the surface potential depends greatly on the resistance of R_1. Figure 7 shows that the speed of the dark decay of the dispersion layer which has the low resistance is high, while that of the dispersion layer which has the high resistance is low; therefore, it is evident that the dark decay depends greatly on the resistance of the layer.

The saturation potential of the layer can not be explained directly from Eq. (1), for the measurements were done by the turn-table method and so the corona discharge was applied on the layer intermittently. Another reason is that the surface potential depends on many complex factors, *i. e.*, the charge density of the corona ions, which are chemisorbed on the layer surface,[16] the injection of electrons from corona ions into the layer, and the orientation of the dipole moment of the binder. Therefore, it is not possible to explain this property from this equivalent circuit model.

The differences in the light decay and in the fatigue effect upon pre-illumination among these polymers' layers can not easily be explained from this model. The only thing we can describe is the experimental results. However, we assume that the photo-phenomena on the surface of titanium dioxide[16] can be explained to some extent by analogy to the case of the zinc-oxide dispersion layer.[17]

The results show that the surface potential of the dark decay decreases proportionally to the square root of the time in the region from 9 min to 80 min. It is impossible to derive the equation in which the surface potential of the dark decay depends on the squre root of the time with the use of the equivalent circuit shown in Fig. 14. Moreover, it is quite significant that this phenomenon appears not only in the dispersion layer, but also in the polymer layer which does not contain titanium dioxide. Inoue proposed an experimental equation in which the decay decreases proportionally to the square root of the time in the zinc-oxide dispersion layer.[9] However, the theoretical meaning of this equation has not yet been clarified. We are now studying the theoretical reason for this time dependency from various viewpoints, but we assume that the diffusion of the corona ions through the layer plays an important role in this phenomenon.

Moreover, it is found in the titanium-dioxide dispersion layer that the logarithm of the surface potential in the dark decay decreases proportionally to the cube root of the time, that it is retained for 4—6 min, and that the period of the proportionality of log V to $t^{1/3}$ depends on the titanium-dioxide content. These phenomena have not been found in the zinc-oxide dispersion layer. It is first time to find such phenomena in the dark decay as electrophotographic properties.

16) T. Iida and H. Nozaki, This Bulletin, **42**, 243 (1969).
17) E. Inoue and T. Yamaguchi, *Electrophotography* **5**, 65 (1964).

These phenomena can not be analyzed easily by the simple model, so we can only describe the experimental results. However, it can be ascribed that there are two different steps in the process of the dark decay of the titanium-dioxide dispersion layer.

The gradient of the dark decay is quite small in the case of the polyvinyl chloride dispersion layer, as is shown in Fig. 10. Therefore, it can be said that polyvinyl chloride is the best material for the electrostatic recording.

At any rate, the corona-charging phenomena of the dispersion layer are quite complicated. We think that the major factors which govern the corona-charging properties are given as follows: (1) the degree of the dispersion between titanium dioxide powder and the polymer, (2) the covering power of the polymer over the surface of titanium dioxide, (3) the chemisorption of corona ions on the layer, (4) the injection of electrons from corona ions into the layer, and (5) the orientation of the dipole moment of the polymer. Therefore, in the future we should study these factors in detail in order to clarify the mechanism of the corona-charging phenomena of the dispersion layer.